J Mater Sci (2010) 45:1137–1142
DOI 10.1007/s10853-009-4065-8

Synthesis, and study of magnetic properties, of $Bi_{1-x}Cd_xFeO_3$

M. B. Bellakki · V. Manivannan

Received: 1 March 2009 / Accepted: 22 November 2009 / Published online: 5 December 2009

Abstract Ceramic $Bi_{1-x}Cd_xFeO_3$ ($x = 0.0$, 0.05, and 0.1) samples were prepared by a citrate-gel method. The as-prepared compounds were calcined at 600 °C for 3 h to obtain nearly single-phase materials. The crystal structure, examined by X-ray powder diffraction (XRD) and Rietveld analysis, confirmed that the samples crystallize in a rhombohedral (space group, *R-3c* no. 161) structure. Magnetic measurements were carried out on the resultant powders from 300 to ~2.5 K. Magnetic hysteresis loops showed a significant increase in magnetization as a result of Cd doping in $BiFeO_3$.

Introduction

Multiferroics, such as $BiFeO_3$ (BFO), exhibit ferromagnetism, ferroelectricity, and ferroelasticity, all in the same phase. They also have promising technological applications in emerging electronic devices such as multiple-state memories and new data-storage media [1–3]. The perovskite $BiFeO_3$ is an attractive material, exhibiting a high Curie temperature ($T_C = 1103$ K) and Néel temperature ($T_N = 643$ K), and weak anti-ferromagnetism at room temperature due to a G-type canted—spin AFM structure [4, 5]. Popa et al. [6] have grown thin films of single-phase $BiFeO_3$ on stainless steel substrate applying a citrate route. The advantages of using citric acid included low recrystallization temperature and the synthesized materials having homogeneous microstructure. They had also shown that, applying a polymeric precursor, nano crystallites of pure $BiFeO_3$ were synthesized [7].

Several attempts to enhance the magnetization in BFO ceramics have been reported in the literature. For example, Wang et al. reported enhanced magnetization in epitaxial BFO film on a (0 0 1) $SrTiO_3$ substrate, which may be attributed to the heteroepitaxial strain, oxygen deficiencies, and enhanced anisotropy [8, 9]. Weak ferromagnetism can also be observed in $BiFO_3$ nanowires and nanoparticles, which may be due to the significant size effects on the magnetic properties of $BiFeO_3$ [10, 11]. Enhanced magnetization due to structural distortion was observed in high-pressure synthesized BFO ceramics [12]. Literature reports indicate that $BiFeO_3$ is doped with both trivalent rare-earth ions and divalent ions [2, 13–16]. Among the divalent dopants, Ca, Sr, Ba, and Pb substitutions in $BiFeO_3$ have been studied extensively [17]. Cadmium is also a divalent metal and its ionic radius is comparable to Ca^{2+}. Recently, it was shown that Cd^{2+} doping in $LaMnO_3$ has tremendously increased the transport and colossal magnetoresistance properties of the materials [18]. However, there is no report in the literature on the study of cadmium-substituted $BiFeO_3$. We report the synthesis of Cd^{2+}-doped BFO ceramics and study the effect of Cd^{2+} doping on structural and magnetic properties.

Experimental

The samples with the composition $Bi_{1-x}Cd_xO_3$ ($x = 0$, 0.05, and 0.1) were prepared by a citrate method [19]. The analytical grade $Bi(NO_3)_2{\cdot}6H_2O$, $Fe(NO_3)_2{\cdot}9H_2O$, and $Cd(NO_3)_2{\cdot}3H_2O$ were used as starting materials. First, we dissolve the equimolar amounts of metal nitrates in ion-free water. The citric acid was then added into the nitrate

M. B. Bellakki · V. Manivannan (✉)
Department of Mechanical Engineering, Colorado State University, Fort Collins 80523, USA
e-mail: mani@engr.colostate.edu

solution such that the molar amount of citric acid was equal to the total molar amount of nitrates in the solution. The solution was then gently evaporated at 80 °C to obtain a homogeneous mixture and dried into gel. The dried powder was then calcined at 600 °C for 3 h in order to get nearly single-phase $BiFeO_3$ crystalline material.

The synthesized samples were characterized for their structure by powder X-ray diffraction (XRD) with a Bruker X-ray diffractometer using Cu K_α radiation with a nickel filter. For Rietveld refinement, the data were collected at a scan rate of 0.5°/min and a 0.02° step size for 2θ from 10° to 100°. The morphology of the powder was examined using a JEOL JSM-840A scanning electron microscope fitted with an energy dispersive X-ray analyzer (EDX). Magnetic measurements were performed with a vibrating sample magnetometer in a physical property measuring system (PPMS, Quantum Design, USA) at an applied field of 3000 Oe.

Results and discussion

Figure 1 shows the powder XRD patterns of $Bi_{1-x}Cd_xFeO_3$ ($x = 0$, 0.05, and 0.1) samples which showed the formation of nearly single-phase nature of these materials. Comparison with the reported pattern in the literature (JCPDF No. 01-070-5668) showed the samples were crystallized in the rhombohedral structure with space group *R-3c*(161). XRD showed the presence of small amounts of the $Bi_2Fe_4O_9$ and $Bi_{25}Fe_2O_{39}$ impurity phases. The structural parameters

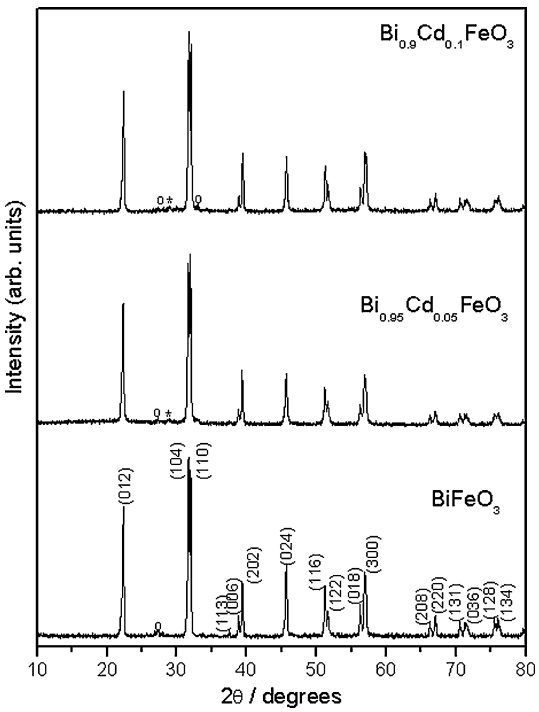

Fig. 1 Powder XRD patterns of $Bi_{1-x}Cd_xFeO_3$ ($x = 0$, 0.05, and 0.1) samples; o and * indicate peaks due to the $Bi_{24}Fe_2O_{39}$ and $Bi_2Fe_4O_9$ phases, respectively

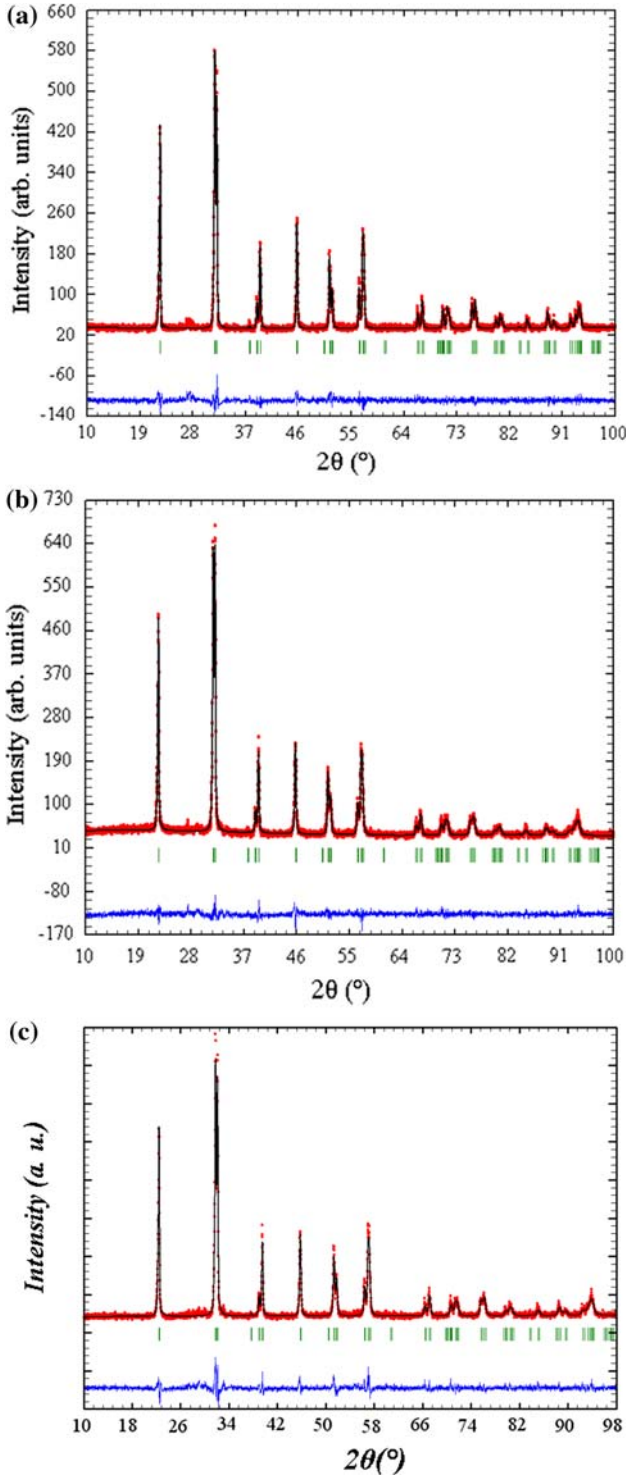

Fig. 2 Typical, observed, calculated, and difference Rietveld-refined X-ray diffraction patterns of **a** $BiFeO_3$, **b** $Bi_{0.95}Cd_{0.05}O_3$, and **c** $Bi_{0.90}Cd_{0.10}O_3$ compounds

were refined by the Rietveld method using the *FullProf* program [20]. The lattice parameters determined for the parent $BiFeO_3$ by the Rietveld method are $a = b = 5.576$ Å, and $c = 13.865$ Å, which is consistent with reported values [21]. In Fig. 2, observed, calculated, and difference XRD patterns as a result of Rietveld refinement of the compounds are given. Figure 2a–c represents the structural refinement results of $BiFeO_3$, $Bi_{0.95}Cd_{0.05}FeO_3$, and $Bi_{0.90}Cd_{0.10}FeO_3$ compounds. There is a good agreement between observed and calculated patterns. No phase transition from rhombohedral to orthorhombic was observed upon Cd^{2+} doping. In Table 1 we summarized structural parameters for doped samples and also we reported the residuals for the weighted pattern R_{wp}, the pattern R_p, Braggs factor R_{Bragg}, structure factor R_F, and goodness of fit χ^2.

SEM pictures of the synthesized materials are presented in Fig. 3. Figure 3a–c shows SEM images of $BiFeO_3$, $Bi_{0.95}Cd_{0.05}FeO_3$, and $Bi_{0.90}Cd_{0.10}FeO_3$ samples, respectively. The particles are agglomerated, and a high interconnection of the grains can be seen from the figure. Particles in both the samples are aggregated into clusters which range from less than a micrometer to about one micrometer in size. EDX results confirmed the Bi/Cd ratio and the stoichiometry of the compounds (Fig. 4).

Table 1 Structural parameters of $Bi_{1-x}Cd_xFeO_3$ ($x = 0$, 0.05, and 0.1) samples

Compounds	$BiFeO_3$	$Bi_{0.95}Cd_{0.05}FeO_3$	$Bi_{0.90}Cd_{0.10}FeO_3$
Crystal system		Rhombohedral	
Space group		*R-3c*(161)	
Lattice parameters			
a (Å)	5.577(3)	5.575(5)	5.574(5)
c (Å)	13.865(6)	13.857(2)	13.856(3)
Cell volume (Å^3)	373.398(1)	372.909(6)	372.910(6)
Bi/Cd			
x	0.0000	0.0000	0.0000
y	0.0000	0.0000	0.0000
z	0.0000	0.0000	0.0000
Fe			
x	0.0000	0.0000	0.0000
y	0.0000	0.0000	0.0000
z	0.2206(3)	0.2209(6)	0.2208(2)
O1			
x	0.4522(9)	0.4689(4)	0.4588(1)
y	0.0259(3)	0.0262(5)	0.0268(1)
z	0.9531(2)	0.9458(6)	0.9474(6)
R factors (%)			
R_P	6.45	5.95	6.95
R_{WP}	8.41	7.64	8.79
R_{Bragg}	4.31	4.44	5.85
R_F	3.70	3.53	3.41
χ^2	0.31	0.30	0.36
Bond lengths (Å)			
Fe–O	1.949(2)	1.956(3)	1.961(5)
Bond angles (°)			
Fe–O–Fe	155.106(3)	156.168(5)	156.172(8)

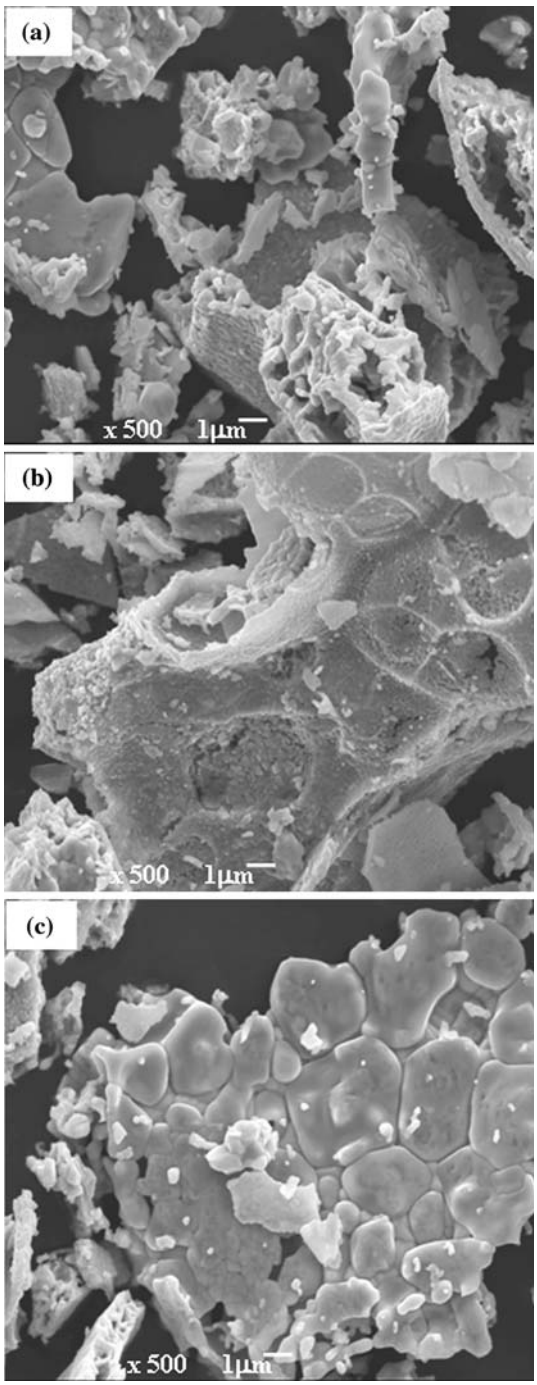

Fig. 3 Scanning electron micrographs of $Bi_{1-x}Cd_xFeO_3$ ($x = 0$, 0.05, and 0.1) samples

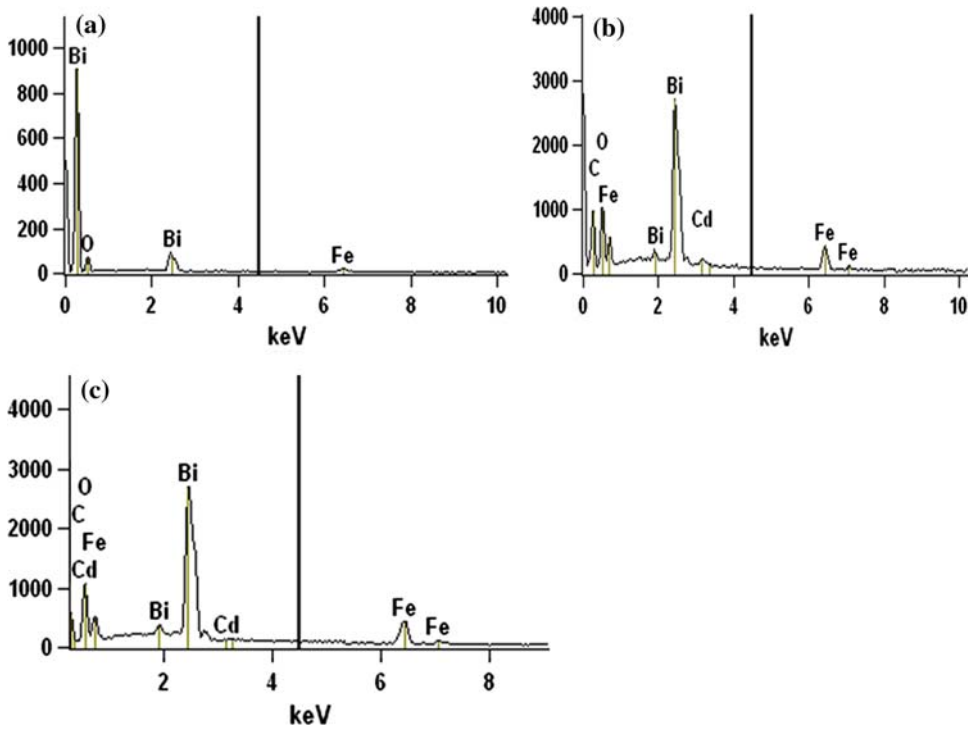

Fig. 4 Micro EDX of $Bi_{1-x}Cd_xFeO_3$ ($x = 0$, 0.05, and 0.1) samples

Effects of Cd^{2+} substitution

It was shown by Kothari et al. [22] that Ca^{2+} doping in $BiFeO_3$ resulted in the release of weak ferromagnetism and created oxygen vacancies and the observed weak ferromagnetism and ferroelectric nature at room temperature indicated the multiferroic nature of these materials. Similarly, Khomchenko et al. [17] have showed that Ca, Sr, Pb, and Ba substitutions at the Bi site resulted in spontaneous magnetization for the $BiFeO_3$ materials. Similarly, Ca^{2+} doped $LaMnO_3$, showed that a corresponding amount of Mn^{3+} is oxidized into Mn^{4+}, resulting in several types of magnetic interactions, among which Mn^{3+}–O^{2-}–Mn^{4+} is a dominant double exchange interaction leading to the ferromagnetic nature of the materials [23].

Cd is also a divalent metal, and its ionic radius is comparable to Ca^{2+} and shown to be promising for improving performance of materials [24]. For example, among all the divalent dopings (Ba, Sr, Ca, Pb, and Cd), $LaMnO_3$ doped with Cd^{2+} showed the best Colossal Magnetoresistance (CMR) performance with more than 80% decrease in resistivity (at 6 T field), a insulator–metal transition (resistivity drop to 86%) [18]. We have shown that Cd doping into $LaFeO_3$ has resulted increased magnetization and magnetic moments of the material [25].

Magnetic measurements were performed on (Bi, Cd)FeO_3 samples, and the results are presented in Fig. 5. Figure 5a shows the evolution of magnetization as a function of applied magnetic M (H) for $BiFeO_3$ and Cd-doped $BiFeO_3$ samples measured at 300 K. All the samples showed a larger loop, indicating a ferromagnetic hysteresis loop, with an increase in magnetization with increased Cd doping. The parent $BiFeO_3$ material crystallizing in a rhombohedral, distorted perovskite structure allows a weak ferromagnetic ordering due to canting of the spins [4, 5]. With Cd doping, (Bi, Cd)FeO_3 samples exhibit enhanced magnetization at room temperature. The increase in spontaneous magnetization could be due to two factors. First, structural disorder due to Cd doping in $BiFeO_3$ orthorhombic perovskite can allow a weak ferromagnetic ordering due to canting of the spins (Cd doping resulted in a Fe–O–Fe bond angle increase from 155.106° to 156.172°) [16]. The structural disorder as a result of Cd doping is evident as shown by the decreasing values of the tolerance factor, t. The value of "t" in general is indicative of the structural stability of perovskite materials, with ideal perovskite materials having a value of 1. The t value decreased from 0.897 for undoped $BiFeO_3$ to 0.893 for 10% Cd doping. Second, Cd^{2+} doping at Bi sites requires charge compensation, which can be accomplished by formation of Fe^{4+} or oxygen vacancies. The statistical distribution of Fe^{3+} and Fe^{4+} (in the case that Fe^{4+} exists) can also lead to net magnetization and ferromagnetism [26, 27]. Magnetization of $BiFeO_3$ is $\sim$0.85 emu/g, which increased to $\sim$0.87 emu/g for 5% Cd-doped $BiFeO_3$ and $\sim$0.96 emu/g for 10% Cd-doped $BiFeO_3$ samples, showing that Cd doping leads to enhanced magnetization in the samples. The increase in magnetization as a result of Cd doping is

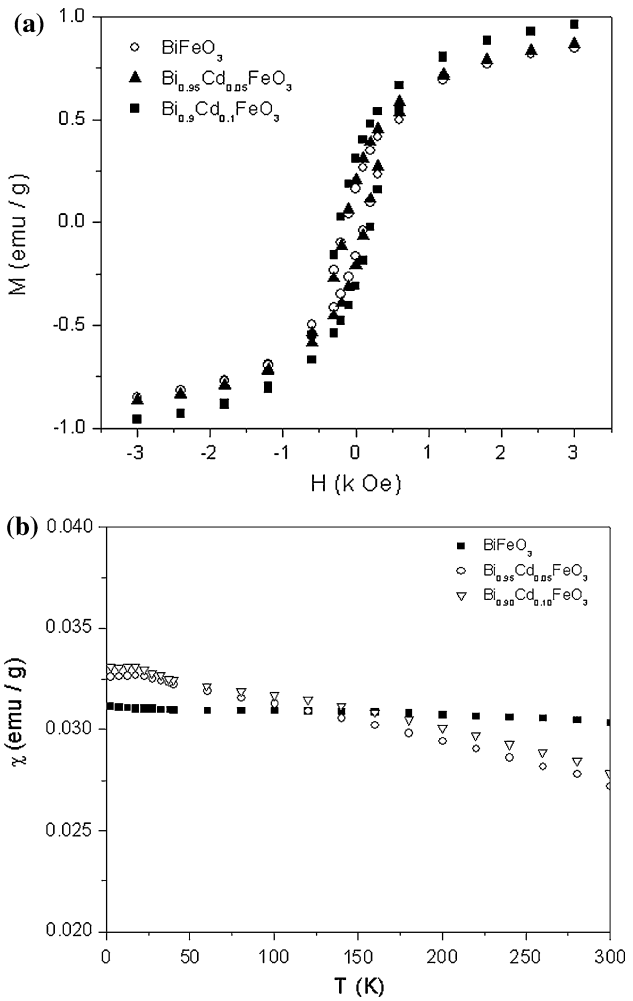

Fig. 5 **a** Magnetization versus magnetic field hysteresis loops for $Bi_{1-x}Cd_xFeO_3$ ($0 \leq x \leq 0.1$) at room temperature. **b** Temperature dependence of the magnetic susceptibility of $Bi_{1-x}Cd_xFeO_3$ ($x = 0$, 0.05, and 0.1) samples

comparable to the best results of divalent doping (ex. Pb or Ba doping in $BiFeO_3$) [17]. Also, the contribution of the $Bi_2Fe_4O_9$ impurity, which undergoes a transition to antiferromagnetic state (around 260 K), has no effect on enhanced magnetization [28]. Figure 5b displays the temperature dependence of the magnetic susceptibility (χ) of $BiFeO_3$ and the Cd-doped $BiFeO_3$ samples. The decrease of χ with decreasing temperature (below 50 K) is indicative of a possible ferromagnetic to antiferromagnetic transition [29].

The magnetic properties of $BiFeO_3$ are largely due to the iron sub-lattice which involved several super exchange interactions such as Fe^{3+}–O–Fe^{3+} or Fe^{3+}–O–Fe^{4+} and determine magnetic ordering. Cd^{2+} doping at the Bi site could induce canting of the antiferromagnetic sub-lattice (with small θ values) leading to weak ferromagnetism. The doping of Cd at the Bi site thus enabled the transition from the nominally spatially modulated spin structure of $BiFeO_3$ into a homogeneously canted one [16, 17].

Though EDX showed the Bi/Cd stoichiometry ratio for the synthesized compounds, there were no significant changes in the lattice parameters obtained from Rietveld structural refinement and magnetic property studies. It is possible that the maximum solid solubility be less than $<10\%$ of Cd, which requires further experimental characterization of the synthesized materials.

Conclusions

Novel Cd-doped $BiFeO_3$ ferrite materials were synthesized by a simple combustion procedure and the structural features were determined and further studied for their magnetic properties. The results showed there is significant increase in magnetization of the parent $BiFeO_3$ as a result of Cd doping, leading to the observed ferromagnetic behavior. Unlike many isovalent dopants, Cd doping in $BiFeO_3$ did not result in any structural phase transition. Structural stability, in conjunction with increased magnetization, positions (Bi, Cd)FeO_3 multiferroic materials for several technological applications.

Acknowledgement The authors thank Prof. Allan Kirkpatrick for his continued help, encouragement, and support.

References

1. Scott JF (2007) Nat Mater 6:256
2. Zhang ST, Zhang Y, Lu MH, Du CL, Chen YF, Liu ZG, Zhu YY, Ming NB, Pan XQ (2006) Appl Phys Lett 88:162901
3. Lee YH, Wu JM, Lai CH (2006) Appl Phys Lett 88:042903
4. Cheng ZX, Wang XL, Ozawa K, Kimura H (2006) Appl Phys Lett 88:132909
5. Cheng ZX, Wang XL (2007) Phys Rev B 75:172406
6. Popa M, Preda S, Fruth V, Sedlackova K, Balazsi C, Crespo D, Calderon-Moreno JM (2009) Thin Solid Films 517:2581
7. Popa M, Crespo D, Calderon-Moreno JM, Preda S, Fruth V (2007) J Am Ceramic Soc 90:2723
8. Wang J, Neaton JB, Zheng H, Nagarajan V, Ogale SB, Liu B, Viehland D, Vaithyanathan V, Schlom DG, Waghmare UV, Spaldin NA, Rabe KM, Wuttig M, Ramesh R (2003) Science 299:1719
9. Ederer C, Spaldin NA (2005) Phys Rev B 71:060401
10. Gao F, Yuan Y, Wang KF, Chen XY, Chen F, Liu JM, Ren ZF (2006) Appl Phys Lett 89:102506
11. Park TJ, Papaefthymiou GC, Viescas AJ, Moodenbaugh AR, Wong SS (2007) Nano Lett 7:766
12. Su WN, Wang DH, Cao QQ, Han ZD, Yin J, Zhang JR, Du YW (2007) Appl Phys Lett 91:092905
13. Lin YH, Jiang Q, Wang Y, Nan CW, Chen L, Yu J (2007) Appl Phys Lett 90:172507
14. Lee D, Kim MG, Ryu S, Jang HM, Lee SG (2005) Appl Phys Lett 86:222903
15. Yuan GL, Or SW (2006) J Appl Phys 100:024109

16. Wang DH, Goh WC, Ning M, Ong CK (2006) Appl Phys Lett 88:212907
17. Khomchenko VA, Kiselev DA, Selezneva EK, Vieira JM, Lopes AML, Pogorelov YG, Araujo JP, Kholkin AL (2008) Mater Lett 62:1927
18. Sahana M, Hegde MS, Vasanthacharya NY, Prasad V, Subramanyam SV (1997) Appl Phys Lett 71:2701
19. Baythoun MSG, Sale FR (1982) J Mater Sci 17:2757. doi: 10.1007/BF00543914
20. Wiles DB, Young RA (1981) J Appl Crystallogr 14:149
21. Chen J, Xing X, Watson A, Wang W, Yu R, Deng J, Yan L, Sun C, Chen X (2007) Chem Mater 19:3598
22. Kothari D, Reddy Raghavendra, Gupta A, Sathe V, Banerjee Gupta SM, Awasthi AM (2007) Appl Phys Lett 91:202505
23. Goodenough JB (1963) Magnetism and chemical bond. Interscience, New York
24. Shannon RD (1976) Acta Crystallogr A32:751
25. Bellakki M, Manivannan V, Das J (2009) Mater Res Bull 44:1522
26. Matsui T, Tanaka H, Fujimura N, Ito T, Mabuchi H, Morii K (2002) Appl Phys Lett 81:2764
27. Mahesh Kumar M, Srinath S, Kumar GS, Suryanarayana SV (1998) J Magn Magn Mater 188:203
28. Cheng ZX, Li AH, Wang XL, Dou SX, Ozawa K, Kimura H, Zhang SJ, Shrout TR (2008) J Appl Phys 103:07E507
29. Li J, Duan Y, He H, Song D (2001) J Alloys Compd 315:259